Electronic Supplementary Material (ESI) for RSC Advances.

Electronic Supplementary Information

Controllable synthesis of Ni-Co-Mn multi-component metal oxides with various morphologies for high-performance flexible supercapacitors †

Pingge He,[a] Qun Huang, [a] Boyun Huang,[a] and Tengfei Chen*[a]

[a]*State Key Laboratory of Powder Metallurgy, Central South University, Changsha 410083, China.*

Calculations:

The specific capacitance of the electrodes is calculated from the charge/discharge curves based on: [1, 2]

$$C_m = (I \times \Delta t) / (\Delta V \times m) \quad (1)$$

where C_m (F g^{-1}) is the specific capacitance, I (A) is the applied current, Δt (s) is the discharge time, ΔV (V) is the potential change after IR drop during the discharge, and m (g) is the mass of active materials.

Coulombic efficiency (η) is the ratio of the number of unit charge inputs during charging compared to the number extracted during discharging, reflecting the charge storage efficiency of electrodes. A low coulombic efficiency is caused by significant loss in charge during secondary reactions, such as the electrolysis of water or other redox reactions in the system.[3] The coulombic efficiency measured in galvanostatic charge/discharge tests is calculated from:

$$\eta = Q_{discharge} / Q_{charge} = I\, t_{\text{discharge}} / I\, t_{\text{charge}} = t_{\text{discharge}} / t_{\text{charge}} \quad (2)$$

Where I is the applied current during galvanostatic charge and discharge.

Fig.S1 shows XPS of NiCoMn2 oxide, containing full element result and detailed high-resolution XPS analyses of Ni 2p, Co 2p, Mn 2p and O 1s, respectively. In Fig. S1a, the peaks located at 49.5, 536.19, 642.3, 808.49 and 870.09 eV correspond to Mn_{3p}, O_{1s}, Mn_{2p}, Co_{2p} and Ni_{2p}, respectively, confirming the presence of Ni, Co, Mn and O elements on the surface of NiCoMn2 oxide. In the O 1s spectrum (see Fig. S1b), two peaks O1 and O2 have been fitted. The O1 at 533.2 eV are associated with C-O functional groups and O2 at 529.2 eV is a typical peak of metal-oxygen bonds.[4] The Ni 2p spectrum is fitted according to two spin-orbit doublets, characteristic of Ni^{2+} and Ni^{3+}, and two shakeup satellites (identified as "Sat.").[5] Similarly, the Co 2p spectrum is fitted with two spin-orbit doublets, characteristic of Co^{2+} and Co^{3+}, and two shakeup satellites.[5] The peaks in the Mn 2p spectrum at 641.5 and 653.2 eV correspond to Mn 2p3/2 and Mn 2p1/2, respectively. However, distinguishing the binding energies corresponding to the oxidation states of Mn^{2+} and Mn^{3+} is rather difficult.[6] Based on the XPS analysis, NiCoMn2 oxide possesses a diverse composition of Ni^{2+}, Ni^{3+}, Co^{2+}, Co^{3+}, Mn^{2+} and Mn^{3+} on the surface, providing more electroactive sites than single- or double-component metal hydroxides.

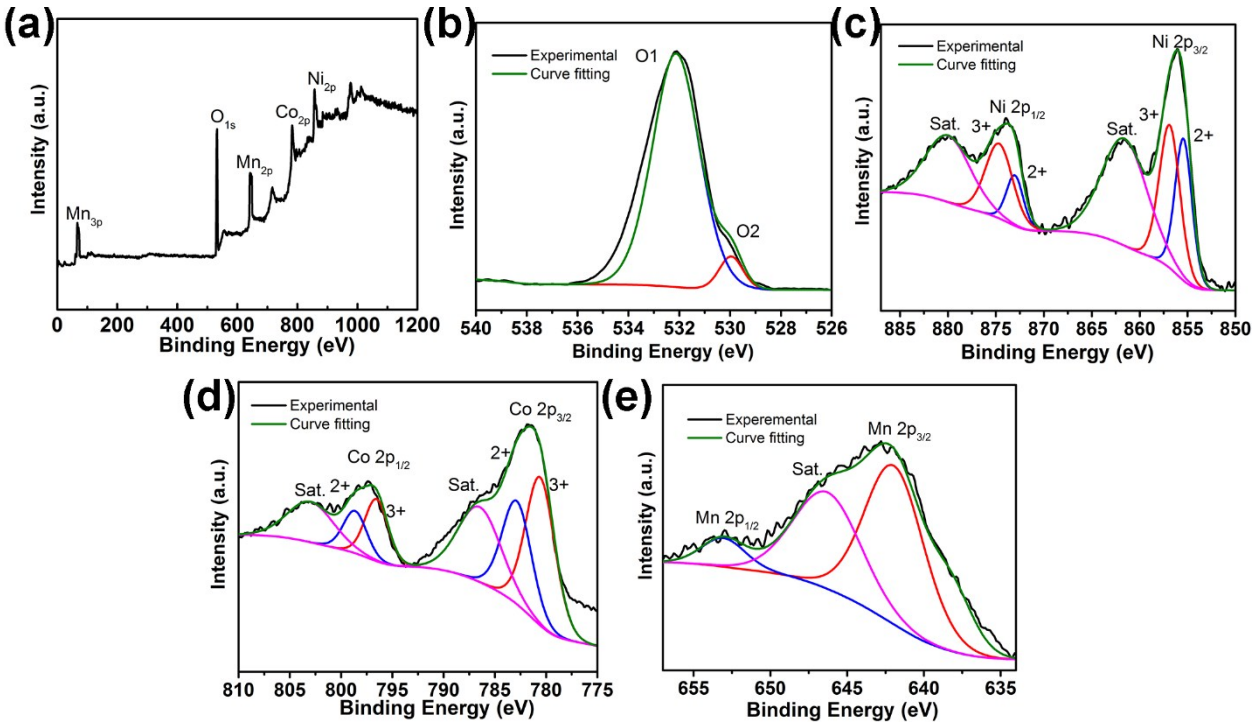

Fig. S1 (a) Full element XPS result. High-resolution XPS spectra of (b) O 1s; (c) Ni 2p; (d) Co 2p; and (e) Mn 2p.

Fig. S2 shows CV curves of metal oxides at scan rates from 10 to 100 mV s^{-1}in a voltage window ranging from -0.2 to 0.5 V vs. SCE.

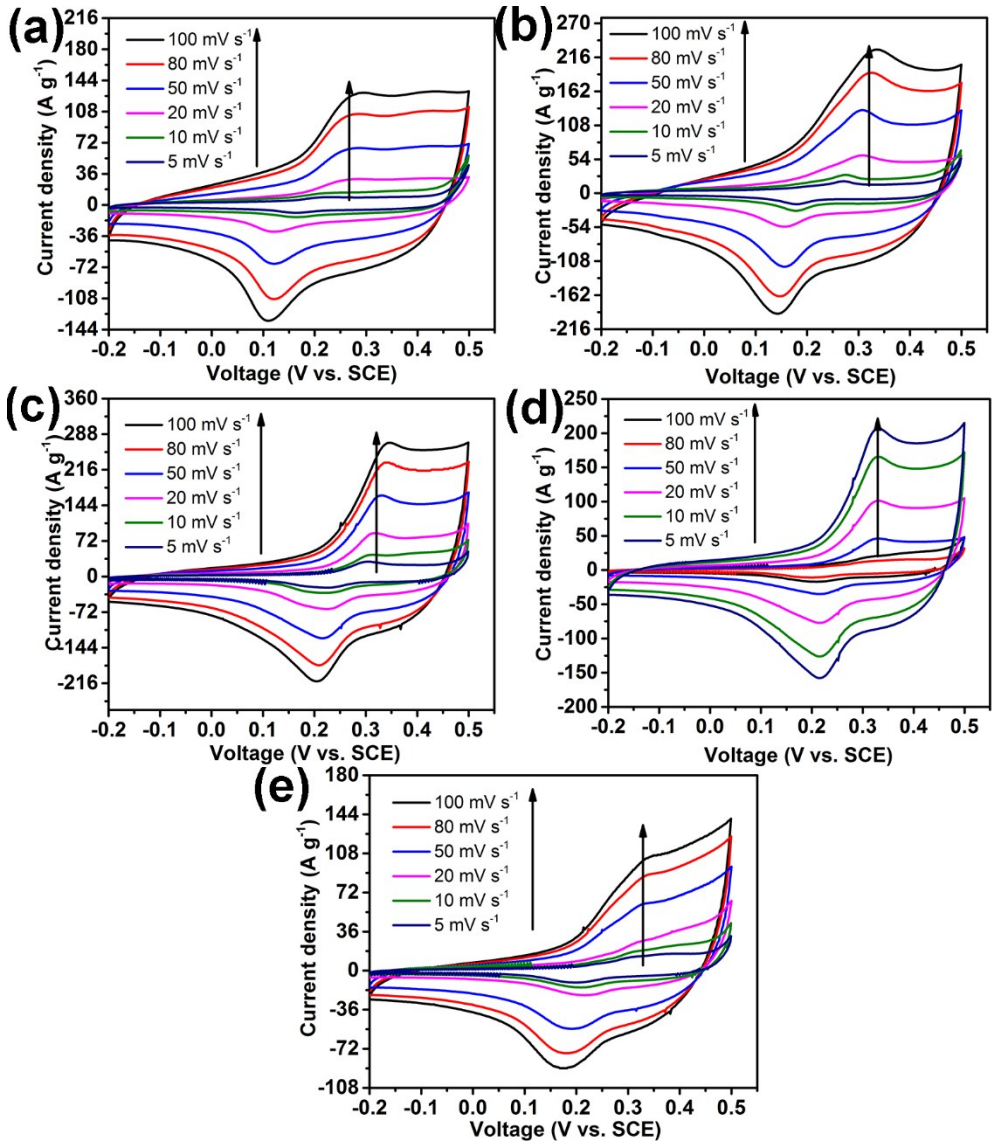

Fig. S2 CV curves of metal oxides at scan rates from 10 to 100 mV s^{-1}. (a) NiCo2; (b) NiCoMn; (c NiCoMn2; (d) NiCoMn3; and (e) NiCoMn5.

Fig. S3 shows the galvanostatic charge/discharge profiles of metal oxides at current densities from 2 to 12 mA cm^{-2} in a voltage window from 0 to 0.5 V vs. SCE.

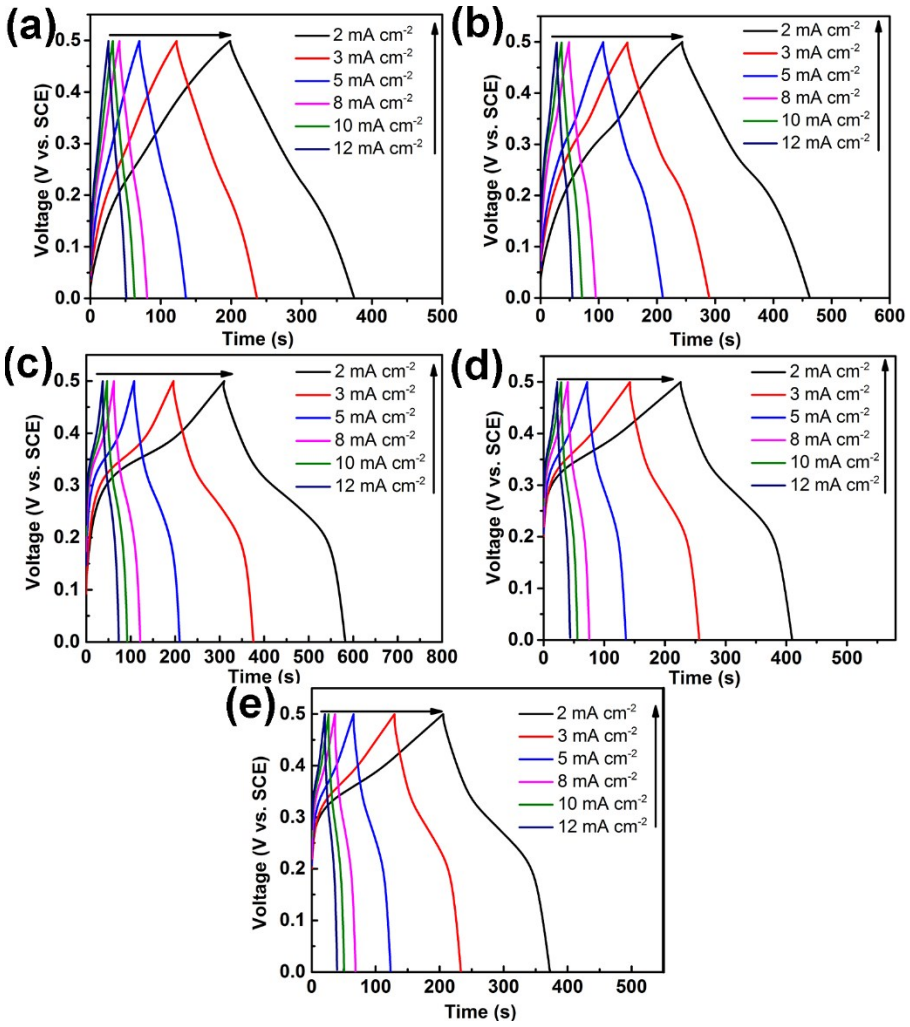

Fig. S3 the galvanostatic charge/discharge profiles of metal oxides at current densities from 2 to 12 mA cm^{-2} (a) NiCo2; (b) NiCoMn; (c NiCoMn2; (d) NiCoMn3; and (e) NiCoMn5.

Nyquist plots of metal oxides recorded from 0.1 Hz to 1 MHz are provided in Fig. S4.

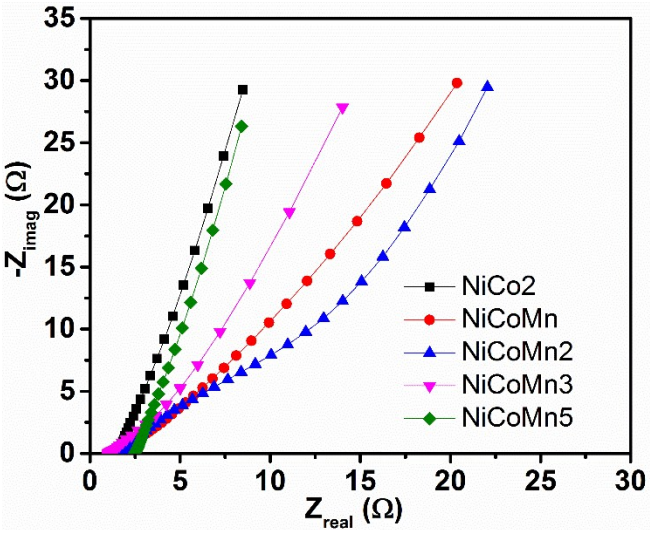

Fig. S4 Nyquist plots of metal oxides recorded from 0.1 Hz to 1 MHz.

Carbon materials are usually by nature hydrophobic. Thus, for the supercapacitor applications, CC was activated to be hydrophilic. The CC is electrochemically oxidized in 1M H_2SO_4 solution through a three-electrode configuration using CC as working electrode, Pt mesh as counter electrode and Ag/AgCl as reference electrode to functionalize the surface with oxygen-containing functional groups. The current and voltage transients during the electrochemical oxidization process are shown in Figure S5.

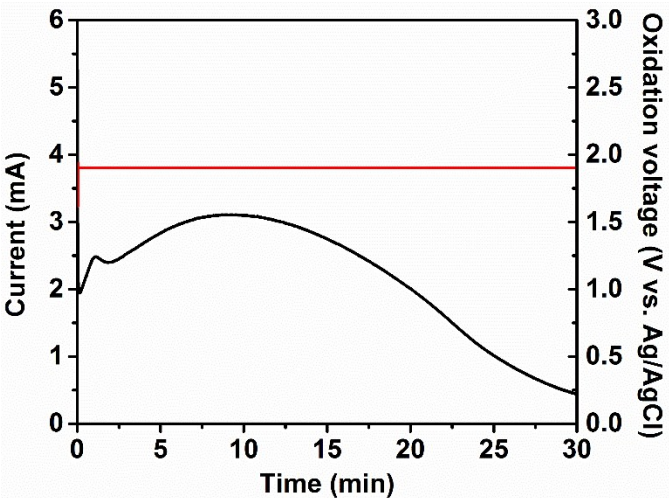

Fig. S5 Electrochemical oxidization process at 1.9 V in 1 M H_2SO_4 for 30 min.

Table S1. A summary of electrochemical performance of state-of-the-art metal oxide-based electrodes.

Electrode materials	Morphology	Substrate	Capacitance ($F\ g^{-1}$)	Cycle life	Ref.
$NiCo_2O_4$	nanowall	carbon cloth	1225	87% (2000 cycle)	[7]
$NiCo_2O_4$	nanoflake	carbon cloth	844	79% (2000 cycle)	[7]
$NiCo_2O_4$	nanosheet	carbon fiber	1338	84.4% (3000 cycle)	[8]
Co-Mn composite	soy pod-like	carbon cloth	832	80% (1000 cycle)	[9]
$MnCo_2O_4$	nanowire	nickel foam	348	92.7% (50 cycle)	[10]
ZnO @$CoMoO_4$	nanorod @nanoplate	nickel foam	1169	109% (5000 cycle)	[11]
$CoMoO_4$/ graphene	nanoparticle	/	394.5	78.4% (500 cycle)	[12]
$NiMoO_4$	nanowire	carbon cloth	414.7	66% (6000 cycle)	[13]
$NiMoO_4$	nanorod	nickel foam	1102.2	90% (1000 cycle)	[14]
Ni-Co-Mn oxides	nanosheet-nanowire	carbon cloth	1434.2	94% (3000 cycle)	this work

Reference

1. P. Simon and Y. Gogotsi, *Nat. Mater.*, 2008, **7**, 845-854.
2. S. L. Zhang and N. Pan, *Adv. Energy Mater.*, 2015, **5**, 1401401.
3. T. Sato, G. Masuda and K. Takagi, *Electrochim. Acta*, 2004, **49**, 3603-3611.
4. J. Marco, J. Gancedo, M. Gracia, J. Gautier, E. Rios and F. Berry, *Journal of Solid State Chemistry*, 2000, **153**, 74-81.
5. B. Cui, H. Lin, Y.-z. Liu, J.-b. Li, P. Sun, X.-c. Zhao and C.-j. Liu, *J.Phys. Chem. C*, 2009, **113**, 14083-14087.
6. S. Bag, K. Roy, C. S. Gopinath and C. R. Raj, *ACS Appl. Mat. Interfaces*, 2014, **6**, 2692-2699.
7. N. Padmanathan and S. Selladurai, *RSC Advances*, 2014, **4**, 8341-8349.
8. F. Deng, L. Yu, G. Cheng, T. Lin, M. Sun, F. Ye and Y. Li, *J. Power Sources*, 2014, **251**, 202-207.
9. J. Gomez and E. E. Kalu, *J. Power Sources*, 2013, **230**, 218-224.
10. L. Li, Y. Q. Zhang, X. Y. Liu, S. J. Shi, X. Y. Zhao, H. Zhang, X. Ge, G. F. Cai, C. D. Gu, X. L. Wang and J. P. Tu, *Electrochim. Acta*, 2014, **116**, 467-474.
11. Y. Cao, L. An, L. Liao, X. Liu, T. Ji, R. Zou, J. Yang, Z. Qin and J. Hu, *RSC Advances*, 2016, **6**, 3020-3024.
12. X. Xia, W. Lei, Q. Hao, W. Wang and X. Wang, *Electrochim. Acta*, 2013, **99**, 253-261.
13. C. Wang, Y. Xi, C. Hu, S. Dai, M. Wang, L. Cheng, W. Xu, G. Wang and W. Li, *RSC Advances*, 2015, **5**, 107098-107104.
14. L. Lin, T. Liu, J. Liu, R. Sun, J. Hao, K. Ji and Z. Wang, *Applied Surface Science*, 2016, **360, Part A**, 234-239.